First Assessment of Mountains on Northwestern Ellesmere Island, Nunavut, as Potential Astronomical Observing Sites

Eric Steinbring[1], Ray Carlberg[2], Bryce Croll[2] Greg Fahlman[1], Paul Hickson[3], Liviu Ivanescu[4], Brian Leckie[1], Thomas Pfrommer[3] & Matthias Schoeck[1]

ABSTRACT

Ellesmere Island, at the most northerly tip of Canada, possesses the highest mountain peaks within 10 degrees of the pole. The highest is 2616 m, with many summits over 1000 m, high enough to place them above a stable low-elevation thermal inversion that persists through winter darkness. Our group has studied four mountains along the northwestern coast which have the additional benefit of smooth onshore airflow from the ice-locked Arctic Ocean. We deployed small robotic site testing stations at three sites, the highest of which is over 1600 m and within 8 degrees of the pole. Basic weather and sky clarity data for over three years beginning in 2006 are presented here, and compared with available nearby sea-level data and one manned mid-elevation site. Our results point to coastal mountain sites experiencing good weather: low median wind speed, high clear-sky fraction and the expectation of excellent seeing. Some practical aspects of access to these remote locations and operation and maintenance of equipment there are also discussed.

Subject headings: site testing

1. Introduction

The cold, dry, dark winter skies of the earth's polar regions are well suited for astronomy. Smooth airflow is aided by a highly stratified atmosphere with strong, stable low-elevation

[1]Herzberg Institute of Astrophysics, National Research Council Canada, Victoria, BC V9E 2E7, Canada

[2]University of Toronto, Dept. of Physics and Astronomy, Toronto, ON M5S 3H4, Canada

[3]University of British Columbia, Dept. of Physics and Astronomy, BC V6T 1Z1, Canada

[4]University of Montreal, Dept. of Physics and Astronomy, QC H3C 3J7, Canada

thermal inversions that persist during the long night. And in particular, extreme latitudes enjoy clear skies and mild winds associated with regions of polar high pressure. In Antarctica, these conditions have encouraged significant focus on the central high-elevation ice plateau (e.g. Saunders et al. 2009; Lawrence et al. 2010, and references therein). This has been aided by a year-round manned presence at the South Pole (latitude 90 South, 2835 m elevation a.s.l.), and more recently Dome C (76S, 3260 m). A permanent station at Dome A (80S, 4200 m), the highest elevation on the plateau, is planned (Gong et al. 2010). In the arctic, as an analogue to the antarctic plateau, the summit of the Greenland icecap (72N, 3200m) has gained interest (Anderson & Rasmussen 2006).

An exciting development in polar astronomy was experimental proof of excellent free-atmospheric seeing at Dome C, Antarctica, with blurring induced by the high atmosphere of only $0\farcs27$ at V (Lawrence et al. 2004). The important implication is that a telescope sited in such conditions can be quite small yet still very productive; a senstivity advantage allowing even a modest, 2-m class optical/near-infrared observatory to be competitive with larger facilities at the current best mid-latitude sites of Hawaii and Chile (Lawrence et al. 2009). However, a concern is that strong boundary-layer turbulence is found to blanket the ice plateau. At Dome C the median seeing 8.5 m above the ice surface is $1\farcs8\pm0\farcs8$ (Agabi et al. 2006), and to take advantage of the free atmospheric seeing there would require a telescope be mounted on a 30-m high tower (Saunders et al. 2008).

An alternate, and more traditional site would be a polar mountain, which would not be subject to the same boundary-layer issues as a flat glacial plateau. Ranges in Canada's Eastern Arctic archipelago are of particular note, having many summits between 1000 m and 2000 m that project into the free atmosphere. None are as high as the antarctic or Greenland icecaps, but Mount Barbeau (82N, 2616 m) on Ellesmere Island, Nunavut, is higher than peaks in northern Greenland, and is almost as high as Cerro Pachon (2715 m) in Chile. And in cold, dry air the effective altitudes of the arctic peaks is increased. Being located as far north as a latitude of 82 degrees they offer the advantage of a longer night, superior to sites further from the poles. This improves the prospects for long time-series observations of, for example, planetary transit searches (Rauer, Fruth & Erikson 2008). The other distinct advantage of a mountain site over an icecap is a solid, rock foundation on which to install a telescope.

Continuous meteorological records going back over 50 years are available for the two year-round manned stations on Ellesmere Island: Alert (82N) and Eureka (80N). All of Ellesmere Island is a polar desert, the coldest and driest in the High Arctic, with annual precipitation less than 9 cm, occuring primarily in summer. Daily climate normals are -40C for winter and 5C in summer. Weather follows a remarkably consistent pattern associated

with the arctic polar vortex, and a strong surface-based thermal inversion persists in the dark: September to March. So during this time the free atmosphere is prevented from mixing, both with lesser latitudes (outside the vortex) and lower altitudes (beneath the surface-based thermal inversion). The arctic polar vortex is not quite as uniform as the antarctic one, though, being generally more elongated and not perfectly centered on the pole, but the region it encircles contains comparably cold, dry, and stable air.

Both Alert and Eureka are accessible year-round by air, and Eureka is supplied annually by ship in summer. Alert is a Canadian military outpost, while Eureka is primarily operated by Environment Canada (EC), a civilian government department. Commercial chartered flights are available to Eureka, generally as combination passenger/cargo operations using Boeing 727 or 737 or smaller turboprop aircraft, all modified for gravel runways. Bushplanes and helicopters supporting scientific research on Ellesmere Island are marshalled at Eureka by Natural Resources Canada through the Polar Continental Shelf Program (PCSP).

Eureka is the furthest north that geosynchronous communications satellites can reliably be used. In fact, Alert is linked to the south through Eureka via six microwave repeater towers. Each is on a high point in a chain along the mountains running the length of the island. The highest of these repeaters (called "Grant", 1256 m) is nearby Alert, with the others along the southeastern flank of the mountains, all accessed by helicopter only. The last is on Black Top Ridge (825 m), to the east of Eureka. The satellite tranceiver is on a 610-m ridge accessible by road, to the west of Eureka. At the top is the Polar Environment Atmospheric Research Laboratory (PEARL), operated by the Canadian Network for the Detection of Atmospheric Change (CANDAC). In 2005/06 this university collaboration redeveloped the previous EC facility, which was decommissioned in the 1990s. It has reliable power - supplied by diesel generators in Eureka - and broadband satellite communications.

This paper outlines our study of selected mountains on the northwestern coast of Ellesmere Island for their use as sites for telescopes, primarily in the optical and near infrared. In 2006 through 2009 four candidate mountain sites were selected for study, and on three of those, meteorological and sky information were gathered (Steinbring et al. 2008; Wallace et al. 2008). The program is described in Section 2, including deployment of site-testing instrumentation in the arctic. The collected data are presented in Section 3 and analyzed in comparison with data from nearby sea-level stations, including Alert and Eureka, one mid-elevation manned site at PEARL, and the highest possible elevation peak on Ellesmere Island. A summary of the results follows in Section 4, with discussion focussing on the practicalities of the sites and the possibility of future development.

2. Site Testing on Ellesmere Island Mountains

A good observing site requires clear skies and a dry, calm atmosphere with the smoothest possible airflow. This generally leads to the selection of a mountain near the sea coast from which the prevailing winds blow with a desert near its base. A high, isolated peak will reduce the influence of upwind terrain. Plus, a higher elevation will result in less air column, lowering precipitable water vapour and improving the expectation of good seeing (Racine 2005). For arctic astronomy, being close to the pole results in lower sun elevations, providing a longer night. Eureka experiences 4020 hours per year when the sun is below the horizon; 2419 hours of nautical twilight or darker (sun-angle < -12 degrees) and 1461 hours of astronomical darkness (< -18 degrees). It is also at sufficiently high latitude to place it within the northern auroral hole; when seen from Eureka, aurora appear low in the southern sky. And a preliminary satellite analysis of Ellesmere Island in winter also pointed to higher clear-sky fraction with increasing latitude and elevation. This will be discussed further in Section 3.

Thus, purely based on geography, the most desirable arctic mountain site will maximize the following four conditions:

- Greatest latitude

- Highest elevation

- Nearest to coast

- Most isolated peak

These criteria quickly point to the mountains of northern Ellesmere Island. They are unique relative to other arctic sites in being true mountains with high prominances, as well as being very near the coast. By comparison, nunataks (rocky areas jutting up from an ice field) although more common on Ellesmere Island, and in some cases significantly higher, would provide less relief above a relatively flat ice surface. These are also more prevalent further inland, not near the coast.

2.1. Preliminary Downselection

As a first step in selecting sites for study, the fourteen highest peaks on Ellesmere Island with latitudes of 80N or greater, within 100 km of the coast and not within an ecologically protected area were identified from digital elevation maps (DEMs).

Next, high-resolution satellite imagery was studied. Mountains nearer the coast had clearly visible exposed rock along their flanks in summertime. So these mountains were considered more accessible but not necessarily having the best sky conditions. For none of the mountains was it possible to determine from either DEMs or images whether a suitably flat area was available for landing a helicopter.

Aircraft are stationed at Alert and Eureka. From there, a one-way flight of 300 km is effectively a limiting range for most helicopters, requiring refueling for the return journey. So near sea level, an area for landing and takeoff of fixed-wing aircraft is also needed - an "unimproved" airstrip sufficient for a bushplane - allowing the cacheing of fuel for helicopter trips and support for a temporary base camp. The availability of suitable locations with unimproved airstrips was discussed with arctic logistics experts familiar with Ellesmere Island. Essentially all of Ellesmere Island could be accessed from Eureka and Alert, although a requirement of access from one or the other, not both, was seen as more efficient. This also pushed towards selecting a group of mountains that could be accessed from the same base camp.

From the initial sample of 14 mountains, a downselection was made based on the following criteria:

- Availability of rock near summit, especially desirable if exposed during summer months

- Possibility of a nearby camp, with a suitable unimproved airstrip

- Proximity to a major research base

- Ability to get permits for testing and potentially for construction

The final consideration has already been partly addressed by avoiding the ecologically protected Quttinirpaaq national park. Further discussion of the process for obtaining permits for scientific research in the Territory of Nunavut will follow in Section 4. The outcome was to focus on the four most northerly mountains in the sample (see Figure 1). Two of these are close to the coast, with two further inland. The inland peaks are somewhat higher (moutain 14 reaches almost 1900 m). All could be accessed by helicopter from a single base camp, supported from Eureka, roughly 250 km to the south.

2.2. Aircraft Access to Remote Locations

Although access to these mountainous locations is possible from spring through fall, the most efficient period is during mid-summer, when daylight lasts 24 hours and nearby aircraft

traffic due to other scientific programs is at its maximum. At this time there has already been significant melting of snow cover, allowing well-cleared landing sites.

The mountain sites themselves must be accessible by helicopter, and to minimize travel the unimproved airstrip and camp should be nearby. The northern fiords of Ellesmere Island present a challenge in this regard, because they can be subject to fog due to onshore winds over patches of open water. This has nothing to do with the quality of the sites themselves, since the fog is confined to the ground, but it restricts travel between the sites and camp and can persist for several days. It is also, therefore, a safety concern as it could lead to a situation where personnel become stranded on a mountain peak. We investigated three possible camp locations nearby the study sites, and used two of those. The best was the most inland, another was along the coast and closer to the sites, and a third - not used - is very near mountain 11. Since we knew in advance which camp location would be used, some fuel was cached there ahead of time, reducing weight on the bushplane when making camp.

To reach remote research sites in the Canadian arctic a de Havilland Twin Otter bushplane is typically used. It is a twin-engined turboprop with large balloon tires that can land on almost any rough airstrip of 200 metres or more. It has a range of 1300 km and takeoff cargo weight of 1100 kg. A larger cousin, the Buffalo, has a payload of over 8000 kg. A commonly used helicopter in the arctic is a Bell 206, a medium-sized single-turbine machine. It has a maximum capacity of either 5 people (including pilot) or about 300 kg near sea-level. A variant with either 7 seating positions or more room for cargo - the 206L "Longranger" - is available, with a similar capacity. Both variants have a range of about 500 km. A somewhat larger machine, the Bell 407, can carry roughly double the load within a similar range.

For helicopters, ceiling and and range decrease sharply with increasing loads. PCSP contracts both Twin Otters and Longranger helicopters for research expeditions in the arctic. It does not normally contract helicopters in the medium to heavy-lift category (lifting 1000 kg to over 5000 kg), but they do operate in the the arctic. Notably, in 2006 a Sikorsky heavy lift helicopter was deployed to recover the BLAST balloon-borne telescope after touchdown on Victoria Island.

2.3. Helicopter-Deployable Instrumentation

The size of helicopter used quickly defines what instrumentation is possible at the sites. The autonomous site-testing stations we deployed, which we have termed "Inuksuit" (plural of inuksuk, the Inuktitut word for the iconic stone waymarkers of the North) are discussed in Steinbring et al. (2008). These battery-powered stations measured basic weather conditions:

air temperature, barometric pressure, relative humidity, wind speed and direction. They also employed a wide-field camera for taking images of the horizon in a fixed direction. Images were taken hourly when batteries were sufficiently charged, typically lasting a few days; a full charge would last about two weeks. Weather records consist of hourly averages from one-minute samples taken at all times. Once per day, when the batteries were sufficiently charged, the stations relayed weather and health-status information via the Iridium satellite network. Because batteries were charged with a wind turbine - a solar array would be useless in the dark, and a sufficiently large bank of batteries to last through the winter impractical - an inherent bias in this approach is to preferentially obtain sky images during windy periods. This bias can be characterized though, as wind speed is recorded, and the system performance well understood. To improve on the state of battery charge, we experimented with a small commercial methanol-based fuel cell.

As a first step in investigating the optical seeing quality of arctic mountain sites, a lunar scintillometer, the Arctic Turbulence Profiler (ATP) has been developed (Hickson et al. 2010). At the moment it is being tested at PEARL, deployed alongside two Sonic Detection and Ranging systems (SODARs). The ATP is designed to be deployed by Bell 206L helicopter later at one of the remote sites. Both it and the SODARs measure turbulence profiles in the planetary boundary layer, within the lower kilometre of the atmosphere. They are not sensitive to high-level turbulence. Another seeing-monitor device is a Differential Image Motion Monitor (DIMM) which measures the overall image quality, but provides no information on what regions of the atmosphere dominate the degradation. It can be combined with a multi-aperture seeing sensor (MASS), which provides information on the height distribution of the image degradation, but is insensitive to ground layer effects. Both MASS and DIMM measurements can be taken with the same small ($\sim$ 0.3 m diameter) telescope, but this is already quite complicated for deployment at a remote site accessible only by helicopter. We have begun investigating operation of a very small (0.1 m) telescope at our sites, which which will be the subject of a later paper.

2.4. Selected Mountain Sites

We opted to employ the helicopter and not fix-winged aircraft for detailed scouting of the sites. The hourly cost is approximately the same, and there is a significant advantage to being able to put the helicopter down immediately on a suspected good site and quickly verify that a landing is possible.

The helicopter pilot has complete control over selecting landing sites, and safety of all aboard is the forefront concern. There were no satellite images of the sites at sufficient

resolution to pre-determine landing sites, whether on rock or snow. In general we found that the best approach was to thoroughly discuss ahead of time with the pilot what locations we considered desirable. It is clear that they kept in mind what characteristics are needed while we performed an aerial search.

In the 2006 field season we installed Inuksuit stations on the two mountains closer to the coast (one station each on 11 and 12). We selected flat rocky areas as high as possible and near the coast. They are along the mountain flanks, below the peaks themselves. One is at 1098 m near peak 11 (designated Site 11A). The other is near peak 12, at 777 m (12A). Both are on the leading edge of long ridges running down to the northwest from the main peaks. That they are rocky and relatively snow-free made helicopter access easier and the solid footing of the stations more assured. The true summits of both of these mountains were scouted and it was determined that they did not provide safe landing sites. They were too sharply peaked to land and so heavily snow-covered that it was not clear how the station could be anchored. Both of the higher peaks (13 and 14) were also thoroughly scouted. Mountain 13 is further inland, the furthest from the initial two sites. Mountain 14 looked the more promising of the two, having a broad saddle and a long snow-covered ridge intersecting the summit, as well as a flatter peak.

In 2007, data from the first year were retrieved, maintenance was carried out on stations at Sites 11A and 12A, a third site within the snow-covered saddle of mountain 14 was selected (Site 14A), and a station installed there. Further maintenance trips occured in 2008, when a small fuel-cell electrical generator was installed at Site 11A, and again in 2009. Measurements of snow depth at Site 14A were made employing a conventional method using an avalanche probe. We also dug bore holes using a power ice-auger. The snow there is about 1 to 3 m deep. The ice below is hard in places, but in layers, which can be bored through with the ice auger. Further tests could be pursued by digging deeper bore holes with a longer ice auger. Based on the surrounding terrain, rock could be just a few metres below the ice, depending on the location.

2.5. Coastal Mountain and Sea-Level Comparisons

Besides Eureka and Alert, the only other meteorological station on the northwestern coast of Ellesmere Island at the time of our downselection in 2006 was at Ward Hunt Island, at sea level. Later sea-level data were taken by other groups during the following two years. One station was at Cape Alfred Ernest, starting in 2007, which was later moved to Milne Glacier in 2008. Both locations are within 50 km of our stations along the coast. The meteorological instrumentation at Cape Alfred Ernest, Milne Glacier, and Ward Hunt

Island are all essentially identical to ours; obtained at 2 m height from ground, whereas ours are closer to 1.5 m. Also, in 2006 the PEARL facility was being being re-commissioned. A standard meteorological tower (at 6 m above ground) was added.

The available data from nearby coastal sites provide useful overlap. Comparisons can also be made with long-term monitoring at Eureka and Alert. A recently published climatology for Eureka goes back over 50 years (Lesins, Duck & Drummond 2009). Apart from sea level stations, PEARL provides records at 616 m elevation, which provides a comparison to our stations at 777 m, 1098 m, and 1639 m, bracketing the peak of the atmospheric thermal inversion. Table 1 gives the locations of the sites and comparisons used in our study.

3.   Observed Weather and Sky Conditions

In general, site-testing requires a multi-year dataset, because year to year fluctuations in nighttime conditions for a given month can be large, and may give a misleading impression. For the arctic, where night lasts several months per year, we consider that data over a significant fraction of one winter period should be minimally sufficient to confirm the expected weather patterns in darkness. But collecting even this comparatively small amount of data has not been an easy task. In the harsh conditions of the arctic, with autonomous stations serviced only in summer, significant gaps in the datasets - weeks to months - are bound to occur. Batteries can get too cold to power the electronics. Thermometer and hygrometer housings are particularly prone to icing and damage. Even with good electrical grounding, buildup of static electricity in dry air is a problem for electronics, sometimes with dramatic consequences. The Inuksuit station at Site 12A was destroyed by this in 2007, burning out much of the electronics, including the weather data-logger. Most of the PEARL data prior to winter 2008 is unusable due to icing, and related mechanical problems. In separate storms during 2008, the entire station at Cape Alfred Ernest was blown down, as was our Inuksuit station at Site 14A.

Figure 4 shows plots of all meteorological and sky quality data for the study locations for over three years beginning in July 2006; symbols follow those used in Figure 3. Corrupted and suspect records, for example, long periods of exactly zero wind speed or wildly varying barometric pressure have been deleted. The Ward Hunt Island station does not have a barometer. Each measured parameter will be discussed in the following sections.

3.1. Nighttime Thermal Inversion

The second and third from top panels of Figure 4 are air temperature and pressure, respectively, for all stations. Dashed lines indicate the average measured pressues; the top dotted black line is mean air pressure at 2616 m for a standard atmospheric model (at 0 Celsius). Here day refers to all samples taken while the sun was above the horizon, and night while below. The strong near-sinusoidal variation of temperature and pressure with sun elevation is evident, and the onset of fall and winter conditions is strongly correlated with sun elevation falling below the horizon. A useful division between seasons then is to refer to all samples taken when the sun is above the horizon as "day" and all while below the horizon "night." In climatology studies this would also be close to a clean division between fall-winter (sun down) and spring-summer (sun up).

As the sun goes down, the winter low-altitude atmospheric thermal inversion quickly develops over much of the High Arctic. It is a remarkably stable phenomenon, intact throughout winter darkness. For Eureka, based on 50 years of balloon soundings, the base of the inversion is almost always at the surface from September through March, with a monthly median depth of about 800 m (Kahl, Serreze & Schnell 1992). At the peak of the inversion profile the temperature is typically 8 to 14 degrees warmer than the surface, which effectively excludes air below the inversion from rising and mixing with the free air above. Interestingly, the lower quartile height during the winter at Eureka is always below 600 m, that is, between 25% and 50% of the time it lies below the elevation of PEARL. The upper monthly quartile in winter for Eureka is below 1200 m. The situation is almost identical at Alert, with inversion depths shifted perhaps 100 m lower. Similar results are obtained for comparable Russian locations (Serreze, Kahl & Schnell 1992), and MODIS satellite results (Liu & Key 2003).

The sharp contrast in air temperature profile relative to day and night is evident in Figure 5, where all station temperature data are plotted relative to barometric pressure. Because barometer data are missing for Ward Hunt Island, the mean temperature for day and night are given at the mean barometric pressure for the same time periods at Alert, which is the nearest with overlapping temporal coverage. Average sping/summer and winter/fall temperature profiles are shown for twice-daily Eureka aerosondes (Lesins, Duck & Drummond 2009). Assuming a consistent temperature profile along the coast, the data are consistent with Site 11A being above the inversion 75% of the time or more at night, and Site 14A always being above the inversion peak.

3.2. Prevailing Winds

Wind speed and direction are given in the fourth and fifth from top panels in Figure 4. For the most part winds at all stations are calm. This is punctuated by interruptions of one to a few days of high winds, with a period of one or two weeks.

The difference between day and night wind speed is not as strong as for temperature. Figure 6 shows the wind speed for all the stations relative to barometric pressure, separated into day and night. One striking feature is the (relatively rare) occurance of very high winds - over 20 m s^{-1} at Alert, Eureka and PEARL. These do not seem to be evident (at least in summer) at Cape Alfred Ernest or Milne Glacier, nor as severe at the other coastal sites. The mean wind speeds for Eureka, PEARL, Site 12A and Site 14A are shown as a connected line; dashed line, median; dotted line, that plus one standard deviation. Median wind speeds are low, below 3 m s^{-1} at all stations, becoming less than 2 m s^{-1} at the higher sites. Figure 7 is a histogram of wind speed for all stations, binned by units of 1 m s^{-1}. In winter, it is evident that Site 11A is less windy than PEARL, and Site 14A seems to be even calmer, although there is less data from which to judge. For comparison, the median nighttime wind speed on Mauna Kea measured during site-testing for the Thirty Meter Telescope (TMT; 2m height at Site 13N) was 3.7 m s^{-1} (Schoeck et al. 2009).

Data from Alert indicates that the prevailing wind in the winter is almost always from the west, which helped focus our attention on the western part of the island. Storms tend to come from the southwest to west along the coast. Moreover, the Lake Hazen area is arctic desert, in the precipitation shadow of the mountains to its west. Eureka has a less obvious prevailing direction, perhaps even being bimodal: south and west. Figure 8 shows histograms of wind direction binned in 10 degree increments, for day and night. At Site 12A winds tend to be southwest to northwest in winter. The dramatic spike in southwesterly winds at Site 14A is influenced by local terrain. The saddle within which the station at Site 14A is located blocks winds from northwest and east to southeast.

3.3. Clear-Sky Fraction

To put our estimates of clear-sky fraction into context, a satellite analysis of sky clarity over Ellesmere Island was first carried out. This was also useful in guiding our initial site selection process. Data from the Advanced Very High Resolution Radiometer (AVHRR) sensor carried on the NOAA polar-orbiting satellites is publicly available as atmospheric parameters via open-source software (http://stratus.ssec.wisc.edu/products/appx/). This provides maps of about 5 km resolution of winter clear-sky fractions, which are high for

northwestern Ellesmere Island. The results for 5 years of 11 μm data beginning in 2000 are shown in Figure 9.

Characterizing sky clarity in nightime polar satellite images is challenging, because there is little contrast between thin cloud and snow. For Eureka, there has been some success in showing from satellite images that ice crystals are blown from higher terrain (Lesins et al. 2009; Bourdages 2009). And it is plausible that this effect is the reason for the low clear-sky fraction (0.10 to 0.25) seen in Figure 9 in the low-lying flat terrain to the south of Eureka and near Lake Hazen, mid-way between Eureka and Alert. Note also the poor visibility in the channel between Ellesmere Island and Greenland, and right at the edge of the northern coast near our sites. At 5 km resolution, this is blurred with pixels that include our sites (some within 5 km of the coast), and so may give values of sky clarity that are too low. This is also pessimistic for another reason, the algorithm used averages over several days, and any thin clouds during that time are considered cloudy conditions during the whole period. Higher spatial resolution data, coincident in time with "ground-truth" observations, will be discussed later, but this preliminary satellite analysis suggested a clear-sky fraction over 60% for isolated mountains. Impressively, this may be better than Mauna Kea (at over 4000 m elevation), which based on SkyProbe data obtained on CFHT, has photometric conditions up to 60% of the time (Steinbring, Cuillandre & Magnier 2009).

The expectation of clearer skies at higher elevations, especially those above the peak of the thermal inversion, are confirmed with recent upward-looking Light Detection and Ranging (LIDAR) measurements from Eureka. These provide a vertical profile of clouds in winter - mostly ice crystals - from laser-backscatter cross-sections. Adopting an optical depth threshold of 0.2 (what astronomers typically refer to as photometric) the fraction of the time clouds were confined to below an altitude of 610 m (the elevation of PEARL) was under 10%, growing to 13% by 1000 m, and 17% by 1500 m (Lesins et al. 2009). The total integrated cloudy fraction was 33% in these March 2006 data. Put another way, less than half the time that it was cloudy (33/17) were those ice crystals at altitudes greater than 1500 m.

All of our horizon camera images were analyzed following the procedures discussed in Steinbring et al. (2008). There were almost 2000 images taken at Site 11A, and a few hundred total at 12A and 14A. The wide field of view allowed good discrimination of cloudy and clear-sky fractions during daylight hours. This camera has an automatic iris, which opens fully under low illumination. Also, the infrared cut-filter automatically retracts, providing imaging with the bare detector. This provided good images until the onset of twilight, but for darker conditions, only data taken when the moon was up and at illuminations greater than 10% were useful (see the top panel of Figure 4). As the moon is up for 24 hours at a time at these

latitudes, much of those periods can be viewed in winter. Visual inspection was adequate for determining the conditions of cloudy, mostly cloudy, mostly clear, and clear. See Figure 10, which shows a sample of 12 sequential hourly images taken when the moon was up. Bright stars were also useful for determining sky clarity, allowing discrimination between a clear sky and uniformly flat overcast, especially if the stars can be seen progressing through the field in successive frames. Some contextual information could also come from illumination of the foreground. Note frames 10 through 12 in Figure 10. The moon brightly reflecting off the snow is a strong indication that the sky is clear, in this case further buffered by stars being visible in the frames.

Visual estimates of cloud cover (in tenths of sky) are made hourly at Eureka. The standard bins used by EC map almost exactly to our horizon-camera data: cloudy, mostly cloudy (over 5 tenths cloud cover), mostly clear (less than 5 tenths, also designated by EC as mainly clear), or clear. A condition of "ice crystals" - often referred to as diamond dust - is not sensed by the horizon camera, although any images of the moon with an obvious halo are deemed cloudy. It is common at Eureka under cold conditions and clear skies. All else are "indeterminant", which for horizon-camera data means either an ice-covered lens or electronically corrupted image, and for Eureka means any other condition besides cloudy, but likely to be so: rain, rain showers, drizzle, snow pellets, snow, blowing snow, fog, freezing fog, snow grains, and snow showers. Eureka can be very cloudy, with conditions less than 30% clear in late summer. However, the intense cold and dryness of winter reduces cloud cover. Water clouds become increasingly rare, with ice crystals dominating. The 50-year climatology for Eureka gives a mean cloudy fraction less than 50% in November through March, so clear-sky fractions something like 50% (some time will be partially cloudy) for most of winter (Lesins, Duck & Drummond 2009).

An issue for our wind-powered Inuksuit stations discussed in Steinbring et al. (2008) is a bias towards obtaining horizon-camera observations during windy periods. That this did not adversely affect our results can be demonstrated by comparing with measurements from Eureka. Figure 11 plots all the horizon camera data against wind speed (average hourly wind speed nearest in time to a sky observation). Small random shifts have been applied to help show the distribution in wind speed. Also plotted are visual estimates at Eureka, transformed to our bins. The median, mean, and standard deviation are overplotted. There is a strong correlation of low wind speeds and clear skies, seen both in the Eureka data (which is not observationally biased to high wind speeds) and our horizon-camera data. Not surprisingly, clear skies are also correlated with high barometric pressure. Figure 12 shows sky clarity data plotted versus pressure relative to mean station pressure.

The duration of clear-sky periods is also comparable to, and perhaps better than Eureka.

For Site 11A, which has the most data of our sites, uninterrupted periods with either mostly clear or clear skies were tallied. The same was done for Eureka, with clear conditions including ice crystals. No observations are made at Eureka at midnight and 1 AM local time, and Site 11A has larger gaps. So all unobserved hours were assumed to have the conditions of the last observation. Each bin of the resulting histogram was multiplied by its associated duration. The results are shown in Figure 13, a plot of the duration-weighted probability of an uninterrupted period of a given number of hours. Site 11A and Eureka show similar trends, both having clear spans of a few hundred hours at a time, although the longest, at 659 hours on Site 11A (almost 4 weeks in May/June 2008) is possibly just a lucky string of shorter periods.

A direct comparison of horizon-camera clear-sky estimates at Site 11A and satellite imagery was also carried out. The satellite analysis was repeated for better 1 km MODIS data with ground coverage of Site 11A when horizon-camera images were taken at similar times. The resulting day and night clear-sky fraction from the Site 11A horizon camera are shown in Figures 14 and 15. Only data taken between fall 2007 and summer 2008 are used here. There are many indeterminant measurements afterwards, and the timestamps are suspect (likely a problem with the computer clock continually resetting) so potentially not accurate to within an hour. The top panel shows the data relative to wind speed. Again, random shifts have been applied to help show the distributions. The bottom panel shows the fraction of observed time in each bin. For nighttime, only those data when the moon was above the horizon and illuminated greater than 10% are shown. To simplify the comparison with satellite analysis, which has just two bins: cloudy or clear, those horizon-camera observations designated mostly cloudy or mostly clear have been combined into one bin termed "transitional." Indeterminant observations (which may be cloudy, transitional, or clear) are accounted for in two separate ways. First, by redistributing them in proportion to median windspeed in the three other bins, which accounts for correlation of clearer skies with lower wind speed, shown as a dashed line. Second, all indeterminant values were deemed cloudy, which is pessimistic, shown as a dotted line. For comparison, the satellite result is shown in red. The horizon camera data seems to agree with the satellite measurements; nighttime skies are clear 60% to 65% of the time at Site 11A.

3.4. Sky Transparency

Under clear skies, sky transparency should be very good on arctic mountain sites. A standard calculation (Hayes & Latham 1975) suggests a mean atmospheric transparency at 1500 m due only to Rayleigh scattering of 0.06 mag at V. An interesting possibility is a

UV window due to ozone depletion (e.g. Brosch 2009). At lower elevations, one issue might be arctic haze, a phenomenon believed to be caused mostly by pollution from Eurasia. It has a thin optical depth, in layers mostly restricted to below the inversion peak (Hoff 1988; Quinn et al. 2007), although this and ice crystals can persist at higher altitudes (Lesins et al. 2009). For longer wavelengths, there is the benefit of little atmospheric water vapour. The cold air saturates, with relative humidities near 100% throughout winter (second-to-bottom panel in Figure 4), resulting in a low, stable water column. The 50-year monthly mean precipitable water vapor (PWV) from December through March in Eureka is below 2 mm, only September and October are higher. This is already comparable to the median measured by TMT on Mauna Kea: 1.9 mm (Otárola et al. 2010). The February quartile in Eureka, when mean PWV reaches a minimum, falls to 1.1 mm, more like the high Atacama plateau in northern Chile (Giovanelli et al. 2001). Eureka is at *sea level*, and a conservative estimate (scaling linearly with pressure) would suggest that Site 14A should have PWV below 1 mm most of the time in winter. Plans are already underway for obtaining PWV measurements at PEARL using an IRMA device.

3.5. Boundary-Layer Seeing

The ATP is designed for deployment at one of the mountain sites, but has obtained some initial data during testing at PEARL. It is based on a lunar scintillometer that UBC has operated successfully at Cerro Tololo (CTIO) for several years, redesigned for operation in the harsh arctic environment. By recording fluctuations in the lunar flux received by photodiodes over a range of baselines, one can reconstruct the C_N^2 profile, and from this determine the seeing as a function of height above ground (Beckers 1993; Hickson & Lanzetta 2004; Hickson, Pfrommer, & Crotts 2008; Tokovinin et al. 2010). A similar device has also been operated on Mauna Kea (MK), and both it and the CTIO results checked against DIMM-MASS.

Close to 12 hours of data were obtained with the ATP, over about 70 hours of operation in fall and late winter 2009/10. Those results are discussed in Hickson et al. (2010), and briefly summarized here. The ground-layer seeing statistics measured by the ATP at PEARL and the PTP at MK are very good. These initial results indicate that the ground layer (GL) at PEARL is weaker than at MK. The median GL seeing is 0″.28 compared to 0″.45 for MK. We must also consider high-level turbulence not sensed by the scintillometer. For MK, the median free atmosphere (FA) seeing is 0″.33 (Schoeck et al. 2009). Adding this to the GL seeing values gives a median total seeing of 0″.46 for PEARL and 0″.59 for MK. However, there is good reason to believe that the FA seeing is better at PEARL than at MK,

as MASS observations from Dome C in Antarctica indicate unusually-weak FA turbulence (Lawrence et al. 2004; Aristide et al. 2009). Like Dome C, PEARL is located inside the polar vortex and may also have weak FA turbulence. In that case, the median total seeing will be less than $0\farcs46$, and lower still at heights greater than 6 m.

4. Discussion

Our intial weather, sky-quality, and seeing data point to good conditions on coastal Ellesmere Island mountains. A strong thermal inversion exists during winter. Peaks over 1000 m are above the peak of this inversion for much of the time. It is also dry, with high clear-sky fractions. Compared to Eureka, clear-sky fractions are higher on coastal mountain sites, with the added benefit of calmer on-shore winds. This may also correspond with improved seeing, something we plan to test. There is already evidence from PEARL that the boundary layer at these locations is weak. Impressively, for all basic site parameters: seeing, clear-sky fraction, PWV, and median wind speed, our results point to Ellesmere Island mountain sites being comparable to or better than Mauna Kea. Detailed characterization of transparency, sky brightness, and seeing are planned for PEARL, although it can already been seen that there is a compelling case for further investigation of the higher mountain sites. For comparison, a summary of weather and site logistics is given in Table 2.

4.1. Site Practicalities

At minimum, we have shown that we can access high-elevation coastal mountain sites on Ellesmere Island. But as is typical in the arctic, changing weather conditions can alter the best-laid plans very quickly. Not only fog, but clouds at the summits have prevented us from reaching the sites. For example, helicopter landings have not been possible for roughly 70% of the trips to Site 14A, leading to delay and increased expense for later return trips. The snow-covered saddle presents no particular challenge; the peak itself is snow-covered too, but possibly workable. For the lower sites, which are on broad, long rocky ridges, helicopter access is more straightforward. Maneuverability around the sites themselves is easy. The ground is covered with boulders about 10 to 50 cm across, and slopes down some distance towards the sea at angles that can be climbed on foot. Even so, a road to the base of either site is not practical, as both are hemmed in by deeply crevassed glaciers.

So far we have relied on a fieldwork plan mapped out with the PCSP field managers that quickly gets us into and out of the field, with a short camp of a few days. A Twin Otter

carries all personnel and equipment to a predetermined unimproved airstrip near the sites. This is done when weather is known to be good, both from satellite images and from reports from nearby camps. Camp is then established, after which a Bell 206L (empty, apart from pilot) rendezvous with us, coming from Eureka. About 3 drums of jet fuel are needed for a Bell 206L helicopter for 10 hours of flying time (including the trip back to Eureka).

As a base camp we have used two different airstrips over four field seasons. The first is closer to the sites but also to the coast and so more prone to fog. The pilots considered it somewhat short. The second is further away from the sites but less prone to fog. It is also flatter, drier and longer than the other. Both have been made safer by filling in some ruts with nearby rocks and marking out the edges with yellow wind markers. A third has been overflown and is quite wet in July, although it may be more workable early in the season, before the melt has progressed. Site 11A is very close to this airstrip, and in fact, is within view from there.

Installing and maintaining equipment at the sites is no more difficult (or any easier) than at other High Arctic locations. We have lost equipment to storms, as have other groups. Communication via the Iridium satellite network has proved effective; calls from the Inuksuit stations when powered (and the antennae operational) was roughly once per week, sufficient to know health status. One route to improving this to the level of obtaining data in real time might be to parallelize the modems, as has been done at remote antarctic locations. Powering our small stations and camera has been the most significant challenge, although we have had reasonably good success using wind. A small fuel-cell electrical generator was tried, with limited success. To get a sense of the feasibility of generating sufficient power for a small telescope, a comparison can be made with the PLATeau Observatory (PLATO) site testing station at Dome A (See Hengst et al. 2008). That uses a bank of 6 single-cylinder diesel engines burning jet fuel. One is kept running at any time, for redundancy, and for waste heat to keep the fuel from gelling in the cold. At its most efficient it can put out about 1 kW, and consumes 300 g kW^{-1} hr^{-1}. For six months operation (assuming start-up at sunset) a similar system for us would require 300 g kW^{-1} hr^{-1} × 1 kW × 4020 hr = 1206 kg, about what a Twin Otter can carry, and at least four trips up the mountain with a Bell 206L. So delivering the fuel is comparable to what our yearly logistics have been so far, and thus seems a reasonable task. Obtaining a land-use permit to operate a diesel generator has not yet been investigated, although it does not violate environmental regulations.

4.2. Possible Development and Future Plans

There is a well-defined process for obtaining permits for scientific studies in Nunavut. Many of these physical studies involve extended camps of many individuals, and the taking of wildlife or rocks and fossils, so a key aim of the permitting process is to regulate the size of camps and environmental impact on the study sites. Another is to respect Inuit land claims and archeological sites. We have a scientific-study permit to test the three mountain sites we have selected and access them from the camp. It is issued by the Nunavut Research Institute (NRI) after review by the Nunavut Impact Review Board (NIRB). This is renewed each year, which involves providing a non-technical summary of the field work, along with a translation into Inuktitut. Our permit is for testing the mountain sites and installing a small telescope, and indicates an end to testing in 2012. It states that, if a larger facility is considered, a new permit will be required.

All research projects funded by PCSP and granted scientific permits by the Nunavut government are subject to screening for an environmental assessment by NIRB. The regulations are the same as federal Canadian regulations. Our project so far falls in a category exempt from assessment. First of all, we are not operating within a national park, which has more stringent requirements. Also, the current stations are temporary, have a footprint less than 25 square metres, do not involve the storage of 4000 litres or more of fuel with 30 metres of a body of water, nor do they involve a field camp exceeding 200 person days. Some other regulations which we are far from exceding, such heights of communications antennae, could trigger assessments as well. Our request for a scientific project permit renewal, after review by NRI, is relayed to the local hamlets and hunter-and-trapper associations (HTAs) for comment. For a site study this is sufficient, as our work is very similar to other research in the area, is not near harvesting areas, and so is not likely to raise concern. The purpose of relaying the permit is to open dialogue, which we welcome. And to help this along, we are encouraged to provide copies of published research to NRI. If a plan for a telescope moves beyond the current feasibility study, a more pro-active approach to consultation is warranted.

The already developed site at PEARL offers an alternative, compromising the best site quality in favor of established infrastructure. A competing site might be Pingarssuit Mountain (77N, 853 m) nearby Thule on Greenland. Solar observations made there in the late 1960s indicated at times "excellent" seeing atop an abandoned radar dome (Janssens 1970) although there is no evidence from the literature that this was followed up with nighttime astronomy. At either of these "low" sites, there are significant advantages to accessibility by road, and the availability of power, communications, and people. Arctic manpower costs are high though, so a telescope at a manned site would still likely be robotic, as it would

necessarily be at a remote site. Any arctic telescope must be engineered to stringent levels of robustness and reliability. So at least for small telescopes, the main disadvantage of the remote sites is the need for deployment and maintenance by helicopter, which although tractable, is expensive.

We have presented an initial observatory site study of northwestern Ellesmere Island, the first concerning arctic mountains. If a premier arctic site could be developed, it would be a compelling location for a wide range of specialized infrared/optical telescopes. And in keeping with the accessibility of the sites in our study, some initial productivity may be possible by deploying a modest telescope. For planet detection this might be quite small, perhaps only 0.1 m in diameter. But this could quickly demonstrate the value of investing in larger facilities, and a plan for a 2-m class telescope with adaptive optics is already being considered for PEARL.

REFERENCES

Agabi et al., PASP, 118, 344

Andersen, M.I. & Rasmussen, P.K. 2006, Astronomy in Antarctica, 26th meeting of the IAU, Special Session 7, 22-23 August, 2006 in Prague, Czech Republic, SPS7, 11

Aristide et al. 2009, å, 499, 955

Beckers, 1993, Solar Physics, 145, 389

Bourdages, L., Duck, T.J., Lesins, G., Drummond, J.R. & Eloranta, E.W. 2009, Atmos. Chem. Phys., 9, 6881

Brosch, N. 2009, Astrophys Space Sci., 320, 207

Eloranta, E.W. & Uttal, T. 2006, 12th Conf. on Atmospheric Radiation, 6.4

Giovanelli, R., Darling, J., Henderson, C., Hoffman, W., Barry, D., Cordes, J., Eikenberry, S., Gull, G., Keller, L., Smith, J.D., & Stacey, G., 2001, PASP, 113, 803

Gong, X., Wang, L., Cui, X., Feng, L. et al., 2010, EAS Publ. Series, Volume 40, 2010, 65

Hayes, D.S. & Latham, D.W. 1975, ApJ, 197, 593

Hengst, S., Allen, G.R., Ashley, M.C.B., Everett, J.R., Lawrence, J.S., Luong-Van, D.M., & Storey, J.W.V., 2008, Proc. SPIE, 7012, 150

Hickson and Lanzetta, 2004, PASP, 116, 1143

Hickson, Pfrommer & Crotts, 2008, in Optical Turbulence: Astronomy Meets Meteorology, ed. E. Maschiadri and M. Sarazin, Imperial College Press, p. 26

Hickson, P., Carlberg, R., Gagne, R., Pfrommer, T., Racine, R., Schoeck, M., Steinbring, E., & Travouillon, T., 2010, Proc. SPIE, in press

Hoff, R.M., 1988, Journal of Applied Meteorology, 27 (2), 125

Janssens, T.J., 1970, Solar Physics, 11, 222

Kahl, J.D., Serreze, M.C. & Schnell, R.C. 1992, Atmosphere-Ocean, 30 (4), 511

Kenyon, S.L. & Storey, J.W.V. 2010, PASP, 118, 489

Lawrence, J.S. et al. 2004, Nature, 431, 238

Lawrence, J.S., Ashley, M.C.B., Bailey, J., Barrado y Navascues, D., et al., 2009, PASA, 26, 379

Lawrence, J.S., Ashley, M.C.B., Burton, M.G., Gillingham, P.R., McGrath, A., Haynes, R., Saunders, W. & Storey, J.W.V., 2010, EAS Publ. Series, Volume 40, 33

Lesins, G., Bourdages, L, Duck, T.J., Drummond, J.R., Eloranta, E.W. & Walden, V.P. 2009, Atmos. Chem. Phys., 9, 1847

Lesins, G., Duck, T.J. & Drummond, J.R. 2009, Atmosphere-Ocean, in press

Liu, Y. & Key, J.R. 2003, Journal of Atmospheric and Oceanic Technology, 20, 1727

Otárola, A., Travouillon, T., Schoeck, M., Els, S., Riddle, R., Skidmore, W., Dahl, R., Naylor, D. & Querel, R. 2010, PASP, 122, 890, 470

Quinn, P.K., Shaw, G., Andrews, E., Dutton, E.G., Ruoho-Airola, T., & Gong, S.L., 2007, Tellus B, 59 (10), 99

Racine, R. 2005, PASP, 117, 401

Rauer, H., Fruth, T. & Erikson, A. 2008, PASP, 120, 852

Saunders, W., Gillingham, P., McGrath, A., Haynes, R., Brzeski, J., Storey, J., & Lawrence, J., 2008, Proc. SPIE, 7012, 151

Saunders, W., Lawrence, J.S., Storey, J.W.V., Ashley, M.C.B., Kato, S., Minnis, P., Winker, D.M., Liu, G. & Kulesa, C. 2009, PASP, 121, 976

Schoeck, M. et al. 2009, PASP, 121, 384

Serreze, M.C., Kahl, J.D. & Schnell, R.C. 1992, Journal of Climate, 5, 615

Steinbring, E., Leckie, B., Welle, P., Hardy, T., Cole, B., Bayne, D., Croll, B., Walker, D.E., Carlberg, R.G., Fahlman, G.G., Wallace, B., & Hickson, P. 2008, Proc. SPIE, 7012, 1

Steinbring, E., Cuillandre, J.-C. & Magnier, E., 2009, PASP, 121, 295

Tokovinin et al. 2010, MNRAS, in press

Wallace, B., Steinbring, E., Fahlman, G., Leckie, B., Hardy, T., Fletcher, M., Pennington, M., Caputa, K., Carlberg, R., Croll, B., Bayne, D., Cole, B., Hickson, P., Pfrommer, T. & Thorsteinson, S. 2008, AMOS Conf. Series, Ed. S. Ryan, 7, The Maui Economic Development Board, 17-19 September 2008

Table 1.   Ellesmere Island Study Locations and Comparisons[a]

Name	Lat. deg N	Long. deg W	Peak elevation m a.s.l.	Station elevation m a.s.l.
Mountain Sites				
11	82.1	83.4	1720	1098 (11A)
12	82.3	82.3	1402	777 (12A)
13	81.9	80.7	1696	n/a
14	82.3	80.5	1868	1639 (14A)
Mountain comparisons				
PEARL	80.0	85.9	610	616
Barbeau Peak	82.1	83.4	2616	n/a
Coastal sea-level comparisons				
Eureka	80.0	85.9		10
Cape Alfred Ernest	82.3	85.5		10
Milne Glacier	82.1	83.4		15
Ward Hunt Island	83.1	74.2		10
Alert	82.5	62.3		31

[a]Ordered by longitude, west to east

Table 2.   Comparison of Sites[a]

Property	PEARL	12A	11A	14A
Physical attributes				
Distance from coast (km)	10	2	9	52
Elevation (m)	616	777	1098	1639
Weather data and observed conditions				
Met. station samples[b]	8584	1200	17837	3856
Sky clarity samples[c]	$\cdots$	470	1983	101
Min. time above peak inversion[d] (%)	25	$\cdots$	75	100
Median wind at night (m s^{-1})	2.6	$\cdots$	1.5	1.1
Practical and logistical issues				
Method of Access	road	helicopter	helicopter	helicopter
Distance to airstrip[e] (km)	15	51	31[f]	70
Time site accessible in summer[g] (%)	100	80	70	30

[a]Ordered by elevation

[b]Hourly averages when all instruments operational

[c]Once-per-hour assessments

[d]Quartile relative to nighttime temperature profile at Eureka

[e]For the remote sites, the further-inland airstrip

[f]Although not used in this project, the nearest airstrip is 7 km

[g]Estimated fraction of time that site was accessible to crew during field work, e.g., a planned trip not having to turn around due to weather
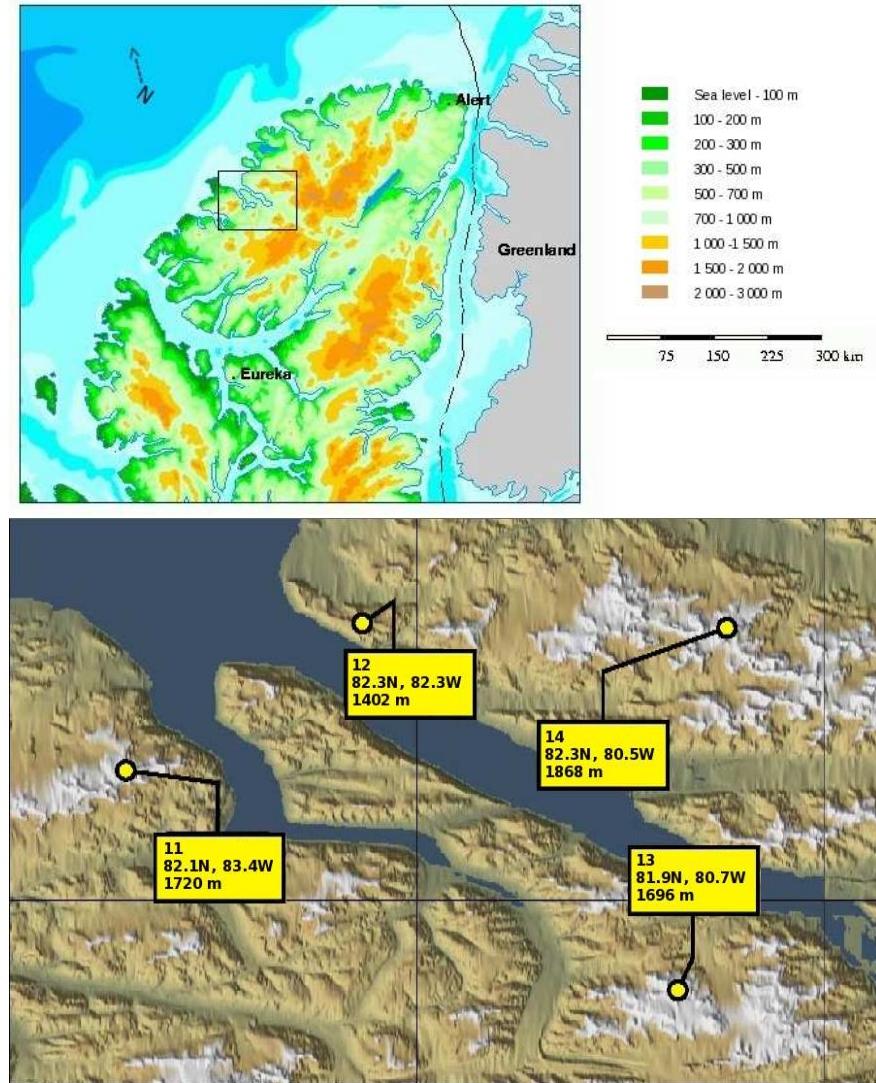
Fig. 1.— Topographic map of Ellesmere Island. The study region is outlined, and below is a higher-resolution map of the selected mountain sites; four isolated peaks over 1000 m within 100 km of the coast. Here white refers to elevations over 1500 m.

Fig. 2.— Images of the Inuksuit station at Site 11A: facing south (top) and north (bottom). Interestingly, the two photos are separated in time by three years; the top image was taken during the day of deployment in 2006, the bottom during the latest maintenance visit in 2009. A thermometer housing is noticeably missing near the base of the wind-turbine tower.
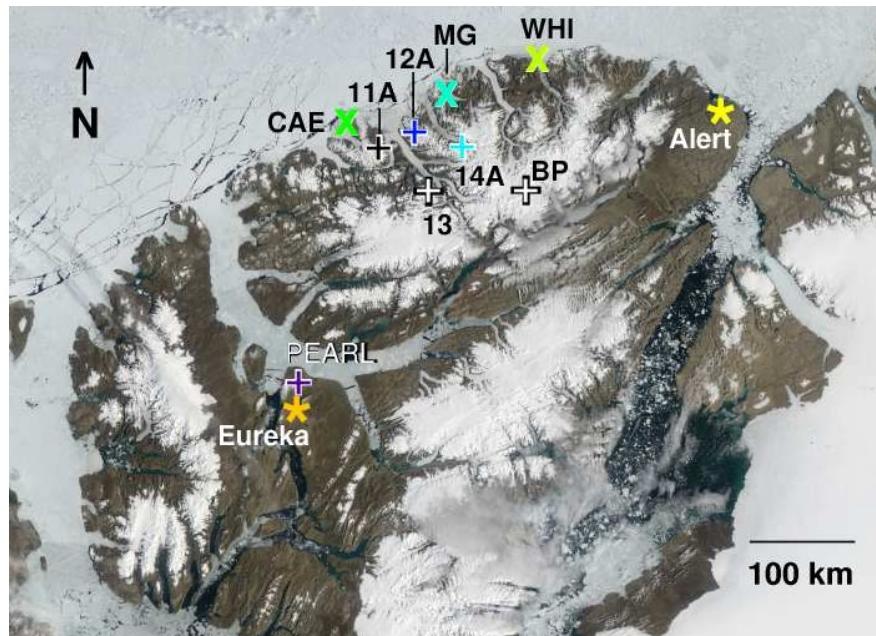
Fig. 3.— Map of Ellesmere Island study locations. Also indicated are coastal sea-level stations at Cape Alfred Ernest (CAE), Milne Glacier (MG) and Ward Hunt Island (WHI); and the highest elevation on the island, Barbeau Peak (BP). Symbols used here are maintained in plots to follow.
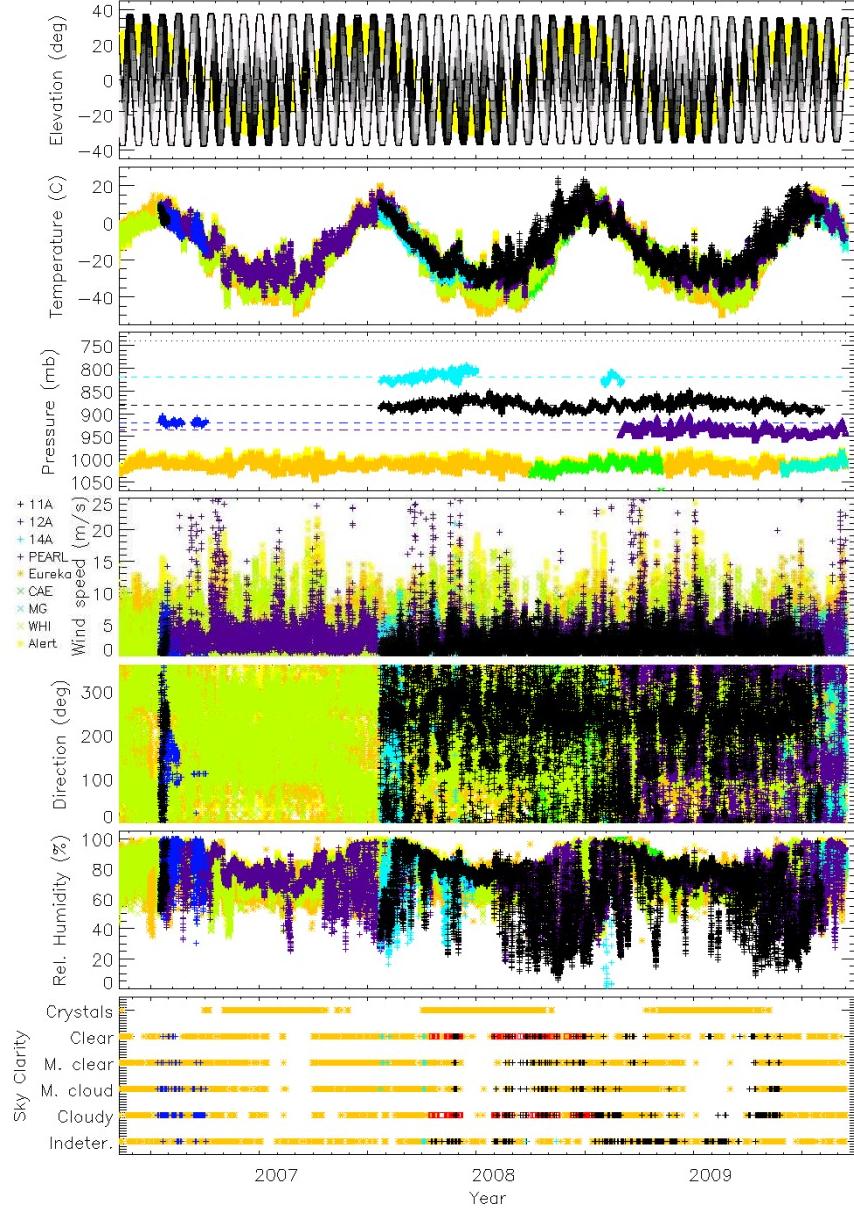
Fig. 4.— Plots of meteorological and sky-clarity data for all stations, starting in July 2006 and continuing until October 2009. Symbols are the same as in Figure 3, red squares indicate satellite sky-clarity assessments discussed in Section 3.3. A plot of sun elevation above the horizon for 80 deg North latitude is shown in the top panel; moon phase and elevation is also indicated; white is 90% or greater illumination, shaded increasingly darker grey down to 10%, beyond which is black.
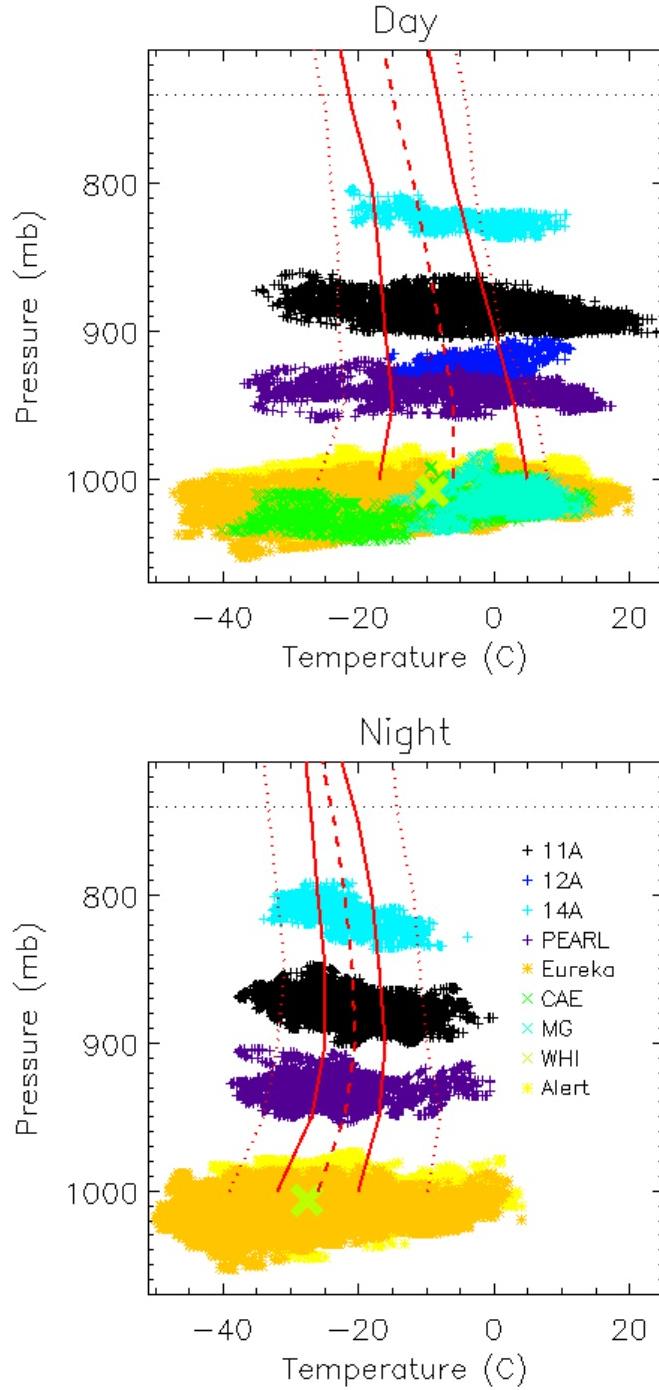
Fig. 5.— Plot of all station barometric pressure data versus temperature, during day (top) and night (bottom); day refers to the sun at or above the horizon, and night to below. Solid red curves are the average sping and summer (day) and winter and fall (night) temperature profiles at Eureka; dashed curves are the averages of day and night; dotted curves, quartiles.
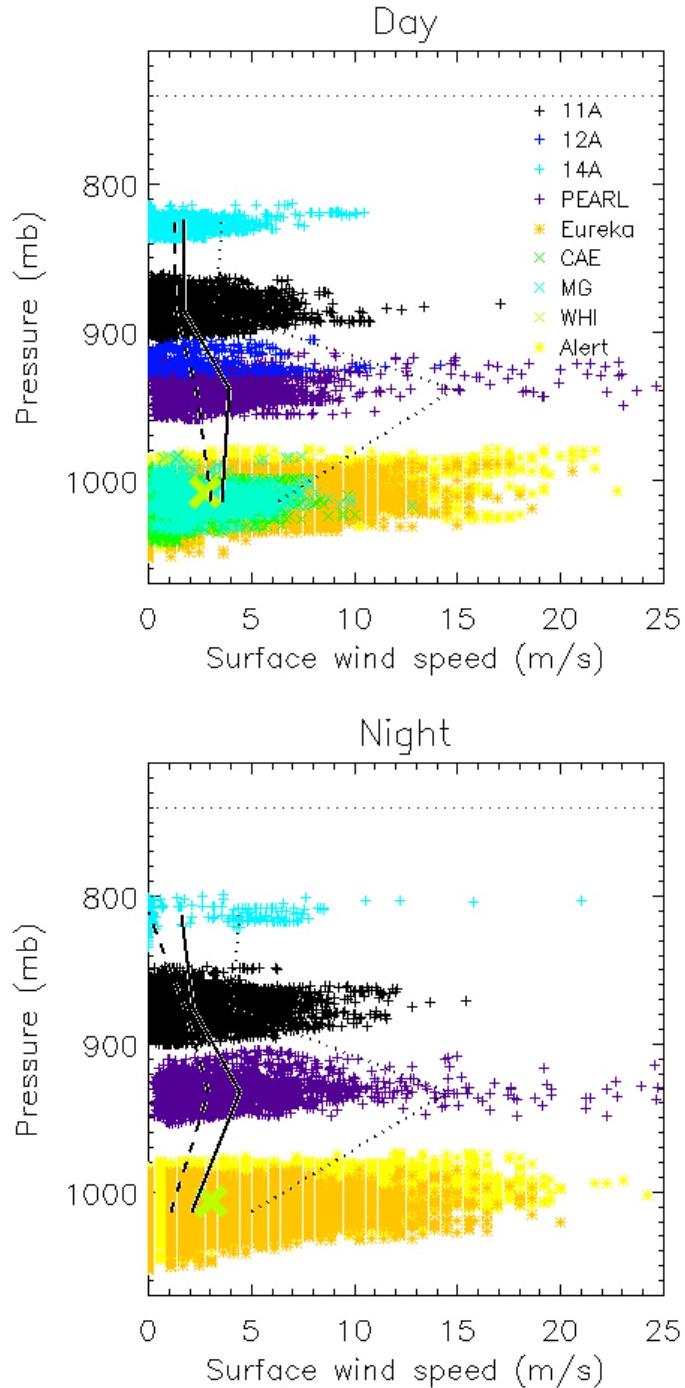
Fig. 6.— Same as Figure 5, except for surface wind speed. Dashed black lines connect the median pressures and wind speeds for Eureka, PEARL, Site 11A, and 14A; solid lines are means; dotted lines are those plus one standard deviation.
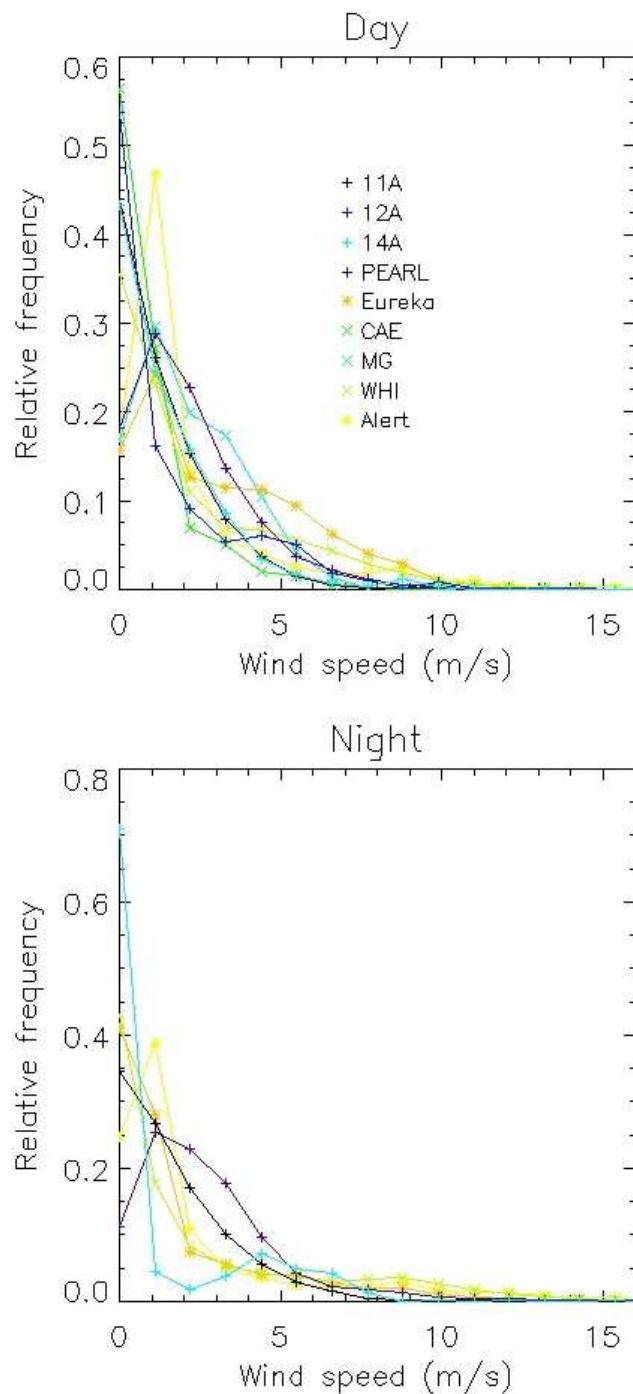
Fig. 7.— Histogram of wind speed for all stations.
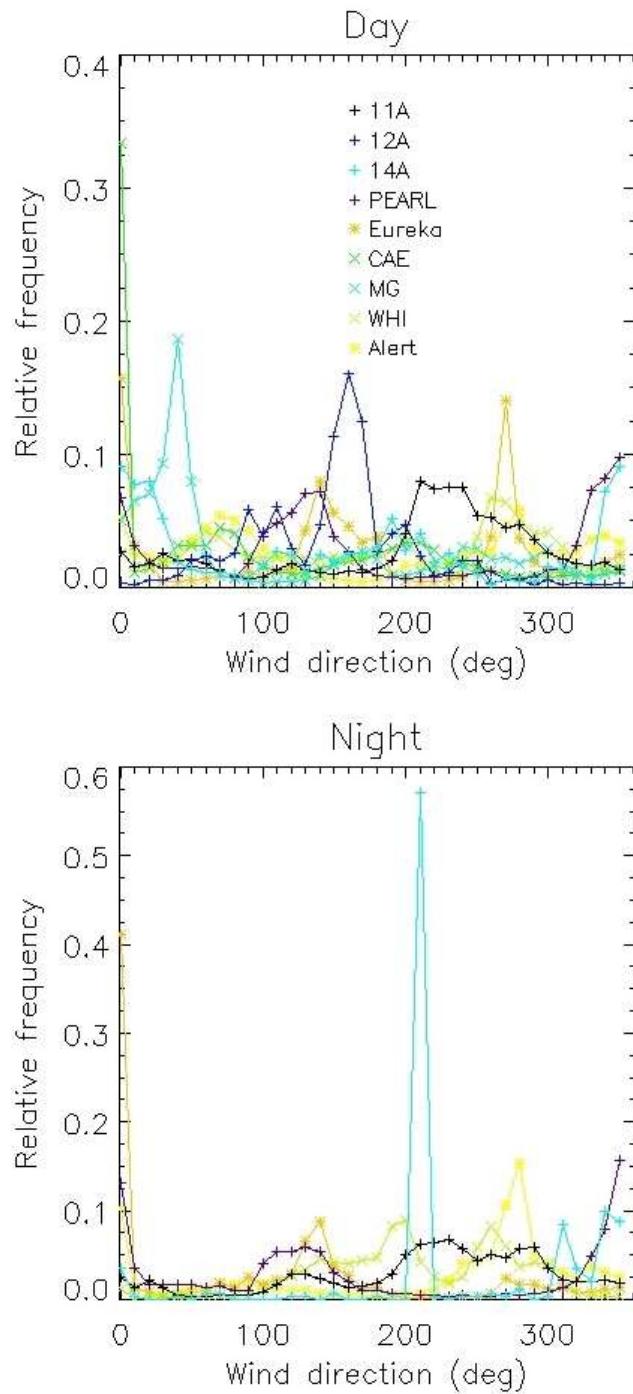
Fig. 8.— Histogram of wind direction for all stations.
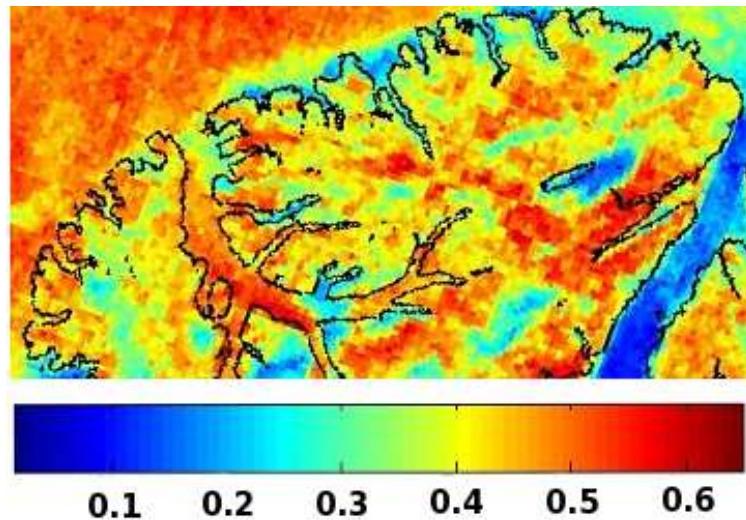
Fig. 9.— Winter clear-sky fraction of time from MODIS data at 5 km resolution. Flat low-lying regions, in the lee of mountains and between Ellesmere Island and Greenland are especially cloudy. Best conditions, over 60% clear-sky fraction, correspond to the highest mountain peaks.

Fig. 10.— Sample nighttime horizon-camera images from Site 11A; 12 sequential hourly images, beginning with cloudy conditions (frame 1), becoming mostly cloudy (2 through 5), mostly clear (6 and 7), and finally clear (8 through 12). The moon is just at the upper edge of the frame in frames 7 and 8; at least one bright star is visible in frames 9 through 12.
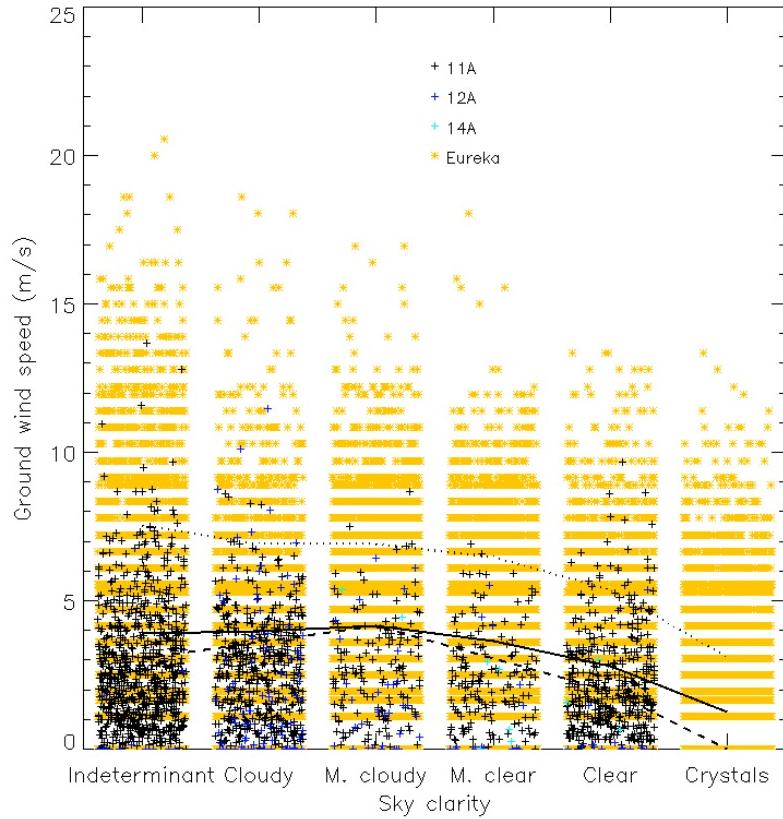
Fig. 11.— A plot showing sky clarity measurements relative to wind speed for Eureka and Sites 11A, 12A, and 14A; symbols are the same as in Figure 8. The condition of "ice crystals" is not represented for the horizon-camera data. Small random offsets have been applied to better show the distribution wind speed. Overplotted are the median (dashed curve), mean (solid curve), and standard devation (dotted curve) for Eureka.
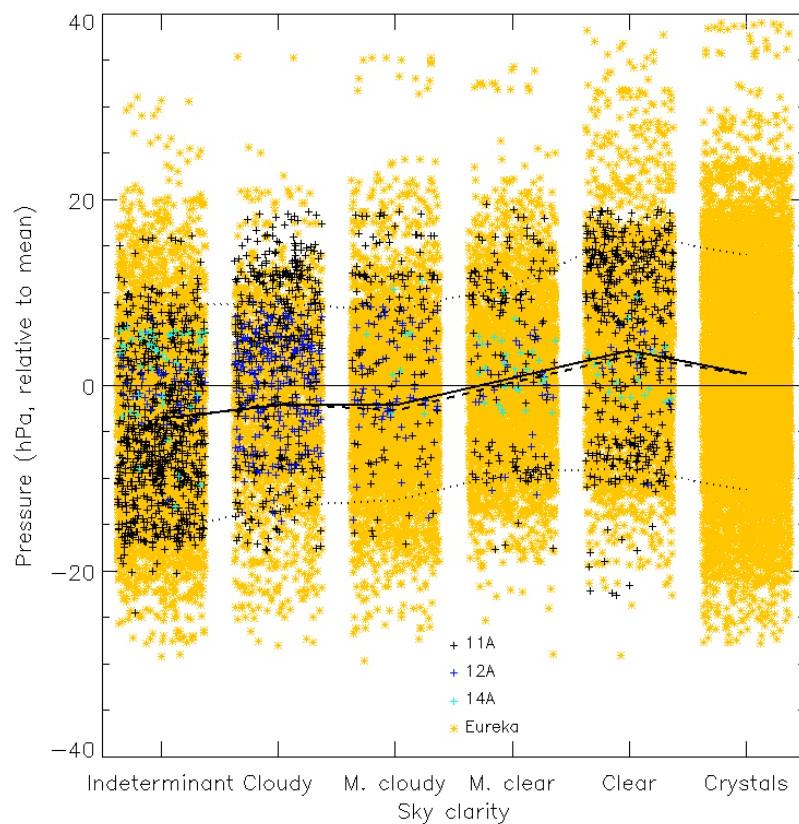
Fig. 12.— Same as Figure 11, except relative to mean barometric pressure.
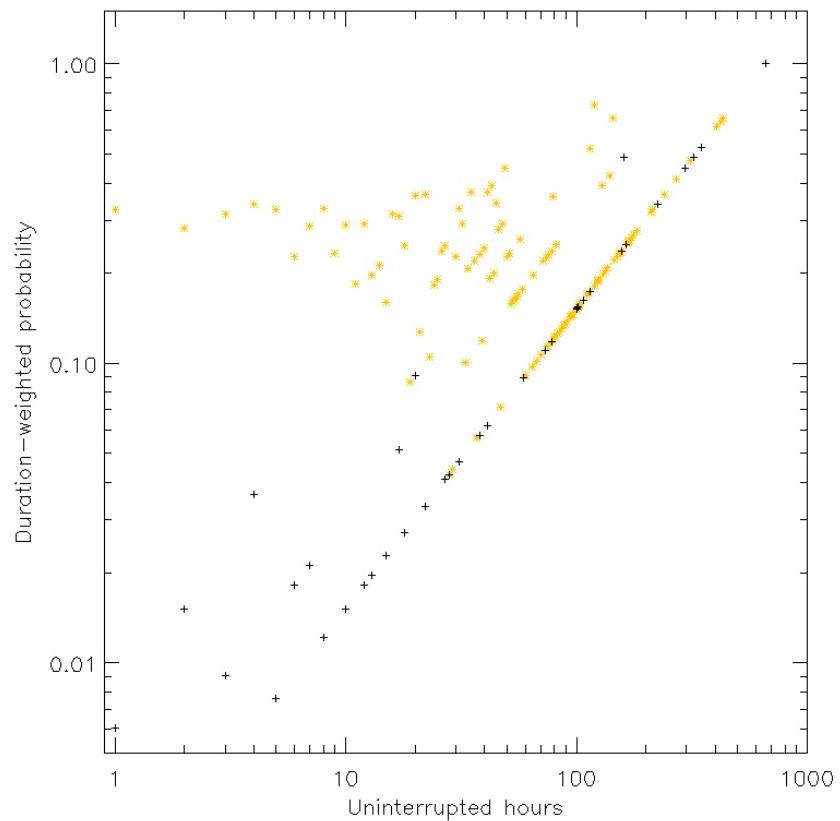
Fig. 13.— Plot of duration-weighted probability of uninterrupted observations of given number of hours during conditions considered mostly clear or clear for Eureka and Site 11A. Eureka assessments include "ice crystals", which for higher elevations would likely be seen as clearer conditions.
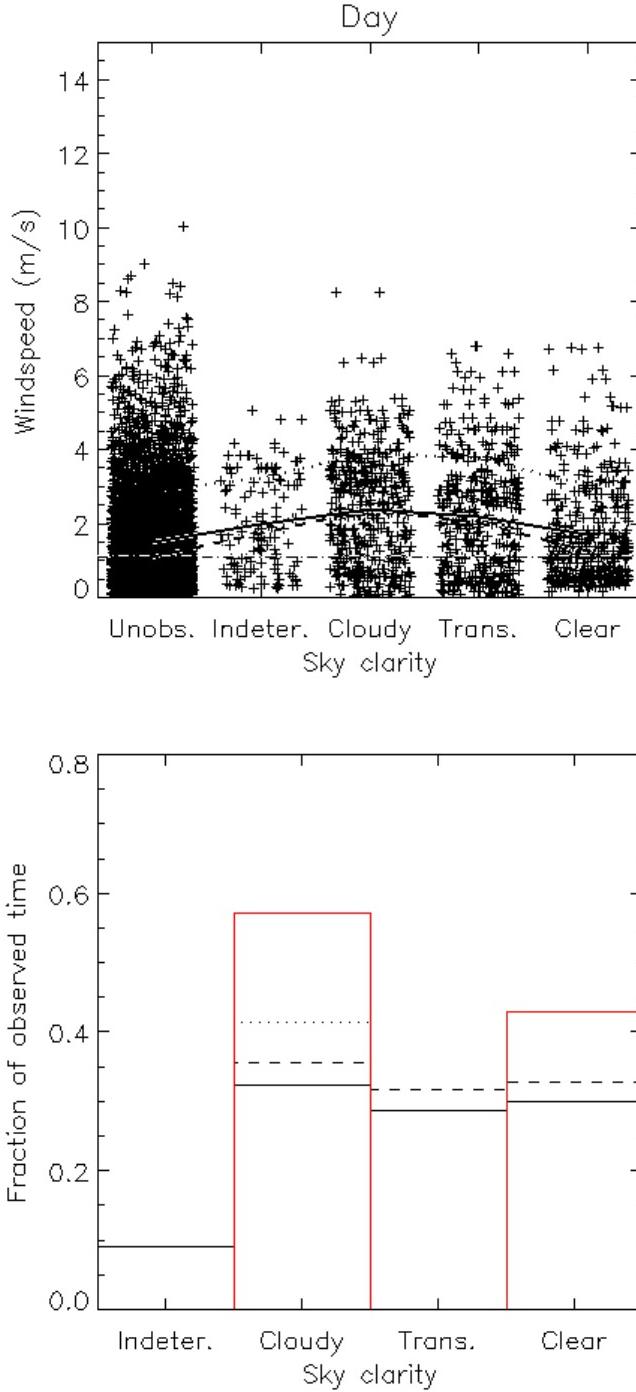
Fig. 14.— Plots of sky clarity during the day for Site 11A relative to wind speed (top) and fraction of observed time (bottom). Overplotted in the upper panel are median wind speed (dashed line), mean wind speed (solid line), standard deviation (dotted line) for each bin, and global median (dot-dashed line). In the lower panel: redistributions of indeterminant samples for wind-speed bias (dashed line), assuming all indeterminants are cloudy (dotted line), and satellite results (red lines).
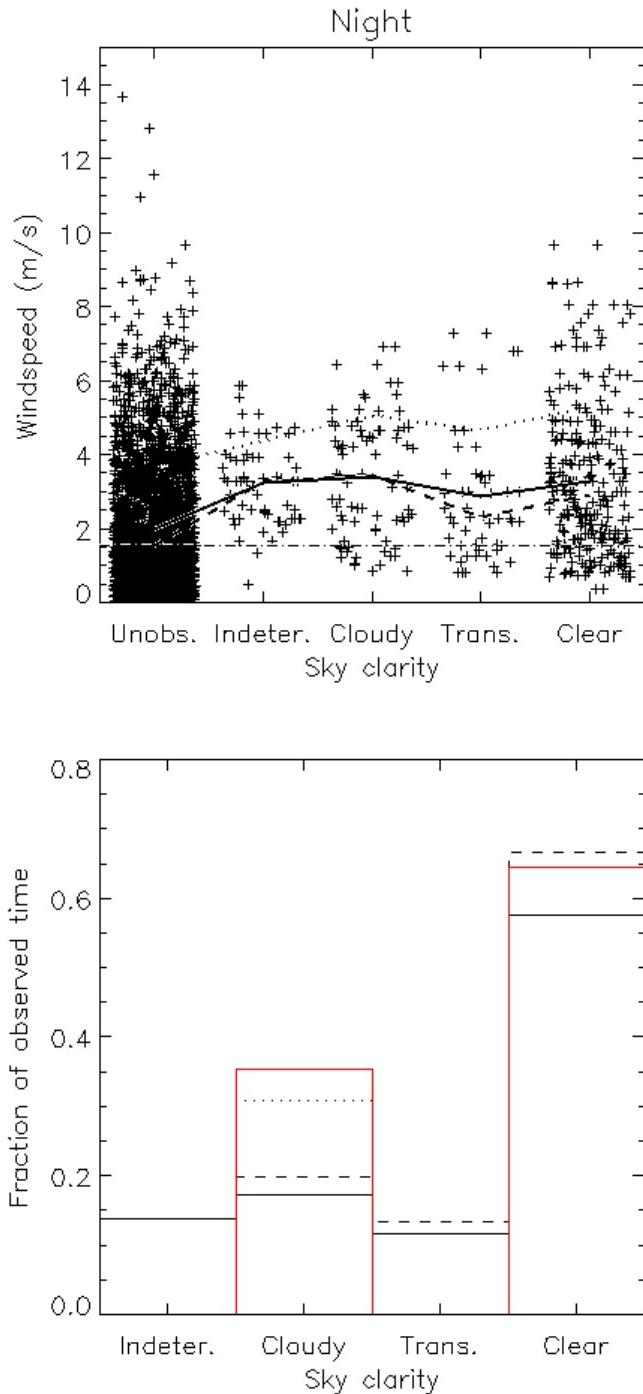
Fig. 15.— Same as 14, except at night. Data taken with moon below the horizon or illuminated less than 10% are considered "unobserved."